Missouri University of Science and Technology
Scholars' Mine

Electrical and Computer Engineering Faculty Research & Creative Works

Electrical and Computer Engineering

01 Jun 2003

Pulse Train™, a Novel Digital Control Method, Applied to a Discontinuous Conduction Mode Flyback Converter

Mark Telefus

Anatoly Shteynberg

Mehdi Ferdowsi
Missouri University of Science and Technology, ferdowsi@mst.edu

Ali Emadi

Follow this and additional works at: https://scholarsmine.mst.edu/ele_comeng_facwork

 Part of the Electrical and Computer Engineering Commons

Recommended Citation

M. Telefus et al., "Pulse Train™, a Novel Digital Control Method, Applied to a Discontinuous Conduction Mode Flyback Converter," *Proceedings of the 34th IEEE Annual Power Electronics Specialist Conference (2003, Acapulco, Mexico)*, vol. 3, pp. 1141-1146, Institute of Electrical and Electronics Engineers (IEEE), Jun 2003.
The definitive version is available at https://doi.org/10.1109/PESC.2003.1216609

This Article - Conference proceedings is brought to you for free and open access by Scholars' Mine. It has been accepted for inclusion in Electrical and Computer Engineering Faculty Research & Creative Works by an authorized administrator of Scholars' Mine. This work is protected by U. S. Copyright Law. Unauthorized use including reproduction for redistribution requires the permission of the copyright holder. For more information, please contact scholarsmine@mst.edu.

Pulse Train ™, a Novel Digital Control Method, Applied to a Discontinuous Conduction Mode Flyback Converter

M. Telefus, A. Shteynberg

iWatt Corporation
90 Albright Way
Las Gatos, CA 95032, USA
Phone: +1/(408)374-4200
Fax: +1/(408)341-0455
E-mail: mtelefus@iwatt.com, ashteynberg@iwatt.com

M. Ferdowsi, and A. Emadi

Grainger Power Electronics and Motor Drives Laboratory
Electric Power and Power Electronics Center
Illinois Institute of Technology
Chicago, IL 60616-3793, USA
Phone: +1/(312)567-8940; Fax: +1/(312)567-8976
E-mail: ferdmeh@iit.edu, emadi@iit.edu

***Abstract*–Pulse Train ™, a new digital control technique for DC-DC converters is introduced and applied to a Flyback converter operating in discontinuous conduction mode (DCM). In contrast to the conventional analog control methods, the principal idea of this new algorithm is to use real time analysis. The proposed technique is appropriate for any converter operating in DCM. However, this work mainly focuses on Flyback converter. In this paper, the main mathematical concept of the new control algorithm is introduced and simulations as well as experimental results are presented.**

I. INTRODUCTION

Conventionally, the output voltage regulation of DC-DC converters has been achieved using frequency domain control techniques. However, real time controllers for power converters enjoy growing popularity due to their accuracy, flexibility, and robustness [1]-[6].

Discontinuous conduction mode (DCM) of operation in a power converter happens when the current of at least one of the inductors reaches zero value before the starting point of the next switching interval [7]. Power converters operating in DCM enjoy higher efficiency as well as lower EMI noise due to the zero current switching of the active devices. Yet, compared to the continuous conduction mode (CCM), the properties of the converters operating in DCM change essentially. For instance, the DC voltage conversion ratio becomes load dependent. Modeling and control of power converters operating in DCM has been the topic of many recent investigations [8], [9].

Implementation of complicated control functions using analog controllers, as the most dominant controllers, is not an easy and sometimes doable task. With the increase of the processing speed of the digital processors on one hand and decrease of their cost on the other hand, digital signal processors have been facing an enormous growth of popularity in control applications in the past few years. Along with the daily advancements of digital IC manufacturing technology, complex control functions are easier to be implemented digitally.

Real time analysis and waveform supervising of the power converters are compatible with the digital control capabilities and do not have the drawbacks of the conventional approaches. In this paper, a new real time control method of power converters operating in DCM to achieve line and load regulation is presented. This method is simple and has been implemented using a digital IC. The control method is robust against the converter parameter variations. Section II introduces the basic concepts of the new control algorithm. Section III investigates the stability of the proposed control scheme. In Section IV, a comprehensive analysis of the output voltage ripple will be presented. Section V discusses the application of a real time zero voltage switching (ZVS) technique for the purpose of efficiency increment. Experimental results of applying Pulse Train technique on a Flyback converter with power factor correction (PFC) are presented in Section VI. Smart skip mode and soft start are discussed in Sections VII and VIII, respectively. Finally, Section IX draws conclusions and presents an overall evaluation of this new control technique.

II. PULSE TRAIN CONTROL SCHEME

Pulse Train control algorithm regulates the output voltage based on the presence and absence of power pulses, rather than employing pulse width modulation (PWM) [10], [11]. Fig. 1 depicts the block diagram of the Pulse Train regulation scheme. If the output voltage is higher than the desired level, *low-power sense pulses* are generated sequentially until the desired voltage level is reached. On the other hand, if the output voltage is lower than the desired level, instead of sense pulses, *high-power power pulses* are generated.

The time duration is the same for the power and sense pulses; but, due to the longer on time of the switch during a power pulse, compared to a sense pulse, more power will be delivered to the load. The ratio between the switch on time of a power pulse and the switch on time of a sense pulse (k) can be chosen by making a compromise between the output voltage ripple and the power regulation range from full power to low power. Additionally, this factor may be updated in an adaptive way to obtain faster transit response or a better performance. Using real time waveform analysis results in ultra fast dynamic response and simplified circuit design.

0-7803-7754-0/03/$17.00 ©2003 IEEE

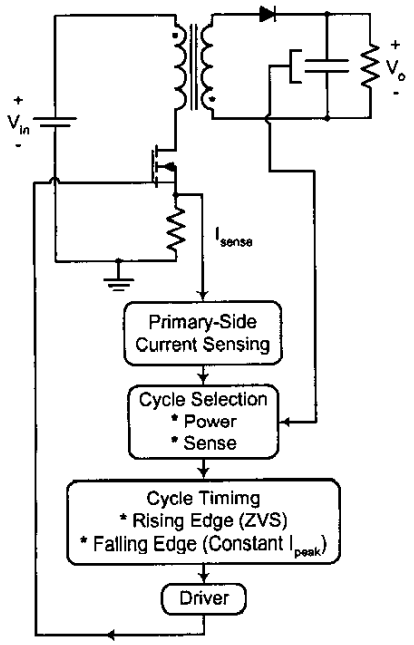

Fig. 1. Block diagram of the Pulse Train control scheme.

Fig. 2 depicts the basic idea of the Pulse Train control technique being applied on a Flyback converter. At the beginning of each switching cycle, based on the difference of the output voltage with the desired voltage level, it will be determined whether there needs a power or sense pulse to be generated. Operating in constant peak current mode control, in a power pulse, the switch remains on and the primary current is allowed to increase until it reaches a designated peak level (I_{max}). At this point, the switch turns off and the next cycle starts when the secondary current reaches zero. A sense pulse has the same period as the preceding power pulse; but, the switch turns off when its current reaches I_{max}/k. Since the primary current ramps linearly with the switch on time, the switch on time of a sense pulse is $1/k$ times as the switch on time of a power pulse. Hence, a sense pulse only transfers $1/k^2$ time as much energy as a power pulse. It is worth to note that the time duration of each sense cycle is equal to the time length of the last power cycle; thus, the converter operates in the fixed frequency mode.

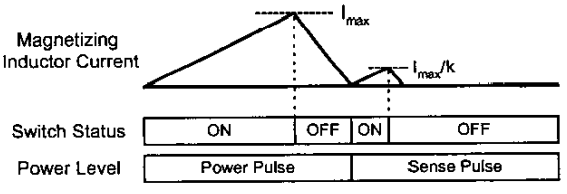

Fig. 2. Power and sense pulse cycles.

Fig. 3 shows the simulation results of applying this control method on a Flyback converter with parameters defined in Table I. For this specific value of the output power demand, the control scheme generates two power pulses and one sense pulse in each regulation cycle.

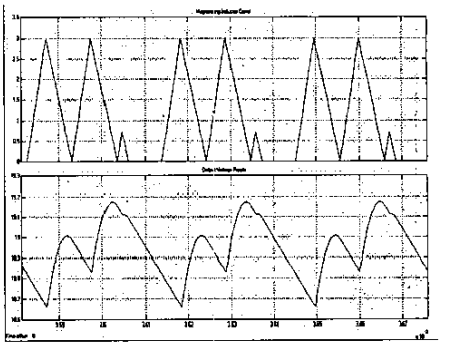

Fig. 3. Simulation results of the Pulse Train control of the Flyback converter.

TABLE I
DEFINITION OF VARIABLES

Variable	Definition	Value
I_{max}	Peak current of the magnetizing inductance	3 A
L	Magnetizing inductance	225 µH
C	Output filter Capacitance	100 µF
R	Load resistance	-
V_{in}	Input voltage	150 V
V_{ref}	Output voltage reference	19 V
t_{on}	on time of the switch in a power pulse	-
t_{off}	off time of the switch in a power pulse	-
T	Switching period	-
k	ratio of the on time of the switch in a power pulse to the on time of the switch in a sense pulse	4
n	transformer turns ratio	6

III. STABILITY ANALYSIS

Without loss of generality, we consider a non-isolated Flyback converter ($n=1$) for the stability analysis. Considering the energy conservation equation in a single period, we can write:

$$\Delta E_C + E_{Load} = \Delta E_S \tag{1}$$

where ΔE_C is the stored energy change of the output capacitor in one period; E_{Load} is the energy delivered to the load during one period; and, ΔE_S is the energy that is drawn from the source in one period. Since the source energy is primarily being delivered to the inductor, equation (1) can be written as:

$$E_{C,(n+1)T} - E_{C,nT} + E_{Load} = E_{L,nT+t_{on}} - E_{L,nT} \tag{2}$$

The integral form of equation (2) can be expressed as:

$$C \cdot \int_{v_{C,nT}}^{v_{C,(n+1)T}} v_C \cdot dv_C + \frac{1}{R} \cdot \int_{nT}^{(n+1)T} v_C^2 \cdot dt = L \cdot \int_{0}^{i_{L,nT+t_{on}}} i_L \cdot di_L \tag{3}$$

Using the trapezoidal rule, we can approximate the energy delivered to the load as:

$$\frac{1}{R} \int_{nT}^{(n+1)T} v_C^2 \cdot dt \cong \frac{T}{2R}\left(v_{C,(n+1)T}^2 + v_{C,nT}^2\right) = \frac{T}{RC}\left(E_{C,(n+1)T} + E_{C,nT}\right) \tag{4}$$

Combining equations (2), (3), and (4) results in:

$$E_{C,(n+1)T} = E_{C,nT} \cdot \frac{1 - T/RC}{1 + T/RC} + \Delta E_S \cdot \frac{1}{1 + T/RC} \quad (5)$$

$$M = \frac{1 - T/RC}{1 + T/RC} < 1 \quad (6)$$

Equation (5) shows the recursive relation of the energy stored in the output capacitor. We need to note that M is always less than one; therefore, the converter is stable under any pattern of power and sense pulses. To have a better understanding of the stability, let's define the reference energy of the output capacitor as:

$$E_C^* = \frac{1}{2} C v^{*2} \quad (7)$$

where v^* is the output reference voltage. Based on the pulse train regulation scheme, we can define the equivalent energy rules as:

$$\begin{aligned} E_C > E_C^* &\Rightarrow \Delta E_S = \frac{1}{2} L I_{\max}^2 \quad \textit{Power Pulse} \\ E_C < E_C^* &\Rightarrow \Delta E_S = \frac{1}{2k^2} L I_{\max}^2 \quad \textit{Sense Pulse} \end{aligned} \quad (8)$$

where k is already defined in Table I. Due to the difference of energy drawn from the power source in power and sense pulses, there are separate sliding surfaces corresponding to each power level. An example of the time-evolution of the sequence of power and sense pulses based on equation (5) is depicted in Fig. 4.

As can be seen in Fig. 4, there are two sliding surfaces. The system has two equilibrium points and the operation is oscillating between the two points. This is exactly the same behavior that we have observed through our extensive simulations and experimental verifications. Both of the equilibrium points are stable. However, the operation between these two sliding surfaces is oscillatory and yet stable. Because of the sliding behavior, there are offsets from the reference signals. The voltage offset, as is presented, is a function of the circuit parameters and does not affect the stability of the system.

IV. Output Voltage Ripple

Stability analysis does not determine the output voltage ripple. Hence, the circuit differential equations need to be solved to predict the output voltage ripple. Considering the Flyback converter, in a power cycle, during the on time interval of the switch, the changes of the output voltage can be written as:

$$\Delta v_{C(on)} \cong -\frac{V_{ref}}{RC} t_{on} = -\frac{V_{ref}}{V_{in}} \frac{L}{RC} I_{max} \quad (9)$$

In the same cycle, assuming that the magnetizing current decreases linearly and output voltage variation is small, the changes of the output voltage during the off time of the switch can be written as:

$$\Delta v_{C(off)} \cong A(e^{-t_{off}/RC} - 1) - RV_{ref} t_{off}/L \quad (10)$$

where we have $A = V_{ref} - nRI_{max} - n^2R^2CV_{ref}/L$ and $t_{off} = LI_{max}/nV_{ref}$.

The total changes of the output voltage after applying a power pulse is the summation of the above two extracted values and can be estimated as:

$$\begin{aligned} \Delta v_{C,P} \cong & \left(V_{ref}\left(1 - \frac{n^2R^2C}{L}\right) - nRI_{max} \right) exp\left(-\frac{LI_{max}}{nRCV_{ref}}\right) \\ & - V_{ref}\left(1 - \frac{n^2R^2C}{L} + \frac{L}{RC}\frac{I_{max}}{V_{in}}\right) \end{aligned} \quad (11)$$

Continuing the same procedure for a sense cycle, we can easily get that:

$$\begin{aligned} \Delta v_{C,S} \cong & \left(V_{ref}\left(1 - \frac{n^2R^2C}{L}\right) - \frac{nRI_{max}}{k} \right) exp\left(-\frac{LI_{max}}{nkRCV_{ref}}\right) - 1) \\ & - \frac{nRI_{max}}{k} - \frac{LI_{max}}{RC}\left(\frac{V_{ref}}{V_{in}} + \frac{k-1}{nk}\right) \end{aligned} \quad (12)$$

$\Delta v_{C,P}$ (solid line) and $-\Delta v_{C,S}$ (dashed line) as a function of the load resistance are sketched in Fig. 5. As we can observe, the control scheme tries to regulate the output voltage by generating the right number of sense and power pulses in each regulation cycle. We can observe that as the output power increases, $\Delta v_{C,P}$ increases; but, $-\Delta v_{C,S}$ decreases. This fact implies that at a higher output power level, the control strategy prefers to have more power pulses rather than sense pulses in each regulation cycle and vice versa in light loads. The value of the output load resistance at which the two graphs cross each other is the value of load, which requires one power pulse associated with one sense pulse in each regulation cycle. Considering different values for the load resistance, different patterns of high and low power cycles can be extracted from the above formulation. Table II shows some examples of this case.

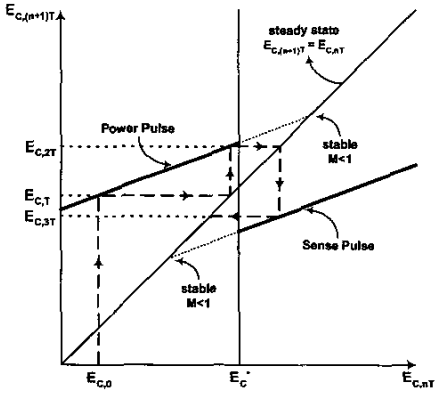

Fig. 4. Sequential evolution of power and sense pulses.

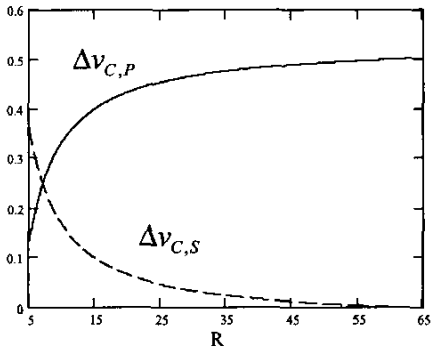

Fig. 5. $\Delta v_{C,P}$ (solid line) and $-\Delta v_{C,S}$ (dashed line) as functions of load resistance in the Flyback converter.

TABLE II
SENSE AND POWER PULSE PATTERN PREDICTION IN ONE REGULATION CYCLE (FLYBACK CONVERTER)

R	Δ_P	$-\Delta_S$	Predicted Pattern
20	0.433	0.066	1*P - 7*S - 1*P - 6*S
15	0.400	0.099	1*P - 4*S
10	0.333	0.165	1*P - 2*S
7	0.249	0.249	1*P - 1*S
5	0.134	0.363	3*P - 1*S - 2*P - 1*S

According to Table II, for instance when $R=10$, we have $\Delta_P \approx 2*-\Delta_S$ which predicts for this value of load, in each regulation cycle, the converter generates two sense pulses associated with each power pulse. So, first we calculate $\Delta v_{C,P}$ and $-\Delta v_{C,S}$ (equations (11) and (12)) associated with each value of R, then we find two integers as this equation holds.

$$\alpha * \Delta v_{C,P} = \beta * -\Delta v_{C,S} \tag{13}$$

Where α and β represent the number of power and sense pulses in each regulation period. During the power cycle, we can express the average value of the diode current as (in a Flyback converter):

$$\overline{i_{D,P}} = nI_{max}(1-d)T/2 \tag{14}$$

where $d=nV_o/(V_{in}+nV_o)$ is the duty ratio. The on time of a sense pulse is $1/k$ of the on time of a power pulse and, hence, we can write:

$$\overline{i_{D,S}} = \overline{i_{D,P}}/k^2 = nI_{max}(1-d)T/2k^2 \tag{15}$$

In the steady state operation, if there are α power pulses associated with β sense pulses in each regulation cycle, then the average value of the diode current is:

$$\overline{i_D} = \frac{\alpha * \overline{i_{D,P}} + \beta * \overline{i_{D,S}}}{(\alpha+\beta)T} \tag{16}$$

By noting that $\overline{i_D} = V_o/R$ and, by solving for the load resistance, one obtains:

$$R = \frac{(\alpha+\beta)V_o}{(\alpha+\frac{\beta}{k^2})\frac{I_{max}}{2}\frac{nV_{in}}{V_{in}+nV_o}} \tag{17}$$

Equation (17) shows how different parameters like input voltage, output voltage, output load resistance, I_{max}, and k affect the pattern of power and sense pulses. This can be used through the design or control process.

V. ZERO VOLTAGE SWITCHING

Sense pulses are being used for extracting additional circuit information, including leakage inductance, transformer reset time, resonant frequency, and secondary diode characteristics. All this information can easily be extracted using an auxiliary winding. These voltage measurements are made on every cycle. If taken from an auxiliary winding, the voltage centers around zero. The auxiliary winding can also provide power for the device.

Fig. 6 shows the effect of a sense pulse on the circuit. Precise measurement of cycle-by-cycle circuit behavior allows zero voltage switching to be performed accurately. Pulse Train achieves zero voltage switching (ZVS) by using the resonance (ringing) that occurs in discontinuous conduction mode Flyback circuits. This resonance occurs after the secondary current falls to zero indicating the transition from power transfer to open-circuit conditions (Fig. 6). The switch is turned on when the voltage across it is at its minimum level reducing turn-on losses. In addition, this switching point is always reached just after the transformer has reset allowing the circuit to operate in critically discontinuous conduction mode, where the switch is turned on immediately after reset, optimizing circuit efficiency, and reducing the size of the transformer.

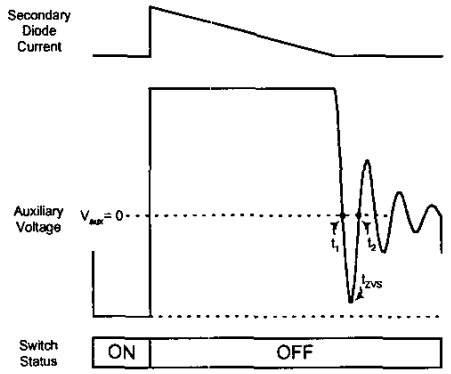

Fig. 6. Auxiliary voltage and zero voltage switching.

As shown in Fig. 6, post-conduction resonance is a damped oscillation that falls very close to zero volts on its first cycle. Zero voltage switching can be achieved very easily, simply by measuring the resonant period on a sense cycle and switching the output transistor when the voltage is closest to zero on the subsequent power cycles. On each power cycle, Pulse Train waits for the auxiliary voltage to drop below zero. This indicates that we are in the post-conduction resonance. After this event, the controller waits an additional ΔT that will take us to the minimum voltage, then turns on the switch for the next power or sense cycle. The time between the zero-crossing on the auxiliary winding and the minimum primary voltage is estimated as being one-half the time between the negative-going zero crossing and the positive-going zero crossing, as shown in Fig. 6. Given the geometry of the

resonant signal, this estimate has high accuracy. This information is already measured during the last sense pulse.

By achieving zero voltage switching, we also achieve critically discontinuous conduction mode because we have turned the transistor back on immediately after the transformer's magnetic field has reset. This eliminates dead time between cycles, fully utilizing the output transformer. As a result, the transformer operates at lower flux levels than conventional converters resulting in lower core losses and, thus, higher efficiency.

Because the waveform is being monitored in real time, critically discontinuous conduction mode is maintained across all variations in line and load conditions. In addition, this method of extracting maximum performance from the inductor is insensitive to component variations since the circuit behavior is measured, not assumed.

VI. Experimental Results

The experimental results of the Pulse Train control method applied to a non-isolated Flyback PFC converter are shown in Figs. 7 and 8. Fig. 7 depicts the switch voltage and inductor current of power and sense pulses for input line voltage of 90 Vac (low line voltage), whereas Fig. 8 shows the same waveforms for V_{in}=130 Vac (high line voltage). This control scheme has also been employed in the implementation of a Flyback PFC converter. Figure 9 shows the rectified sinusoidal input voltage and the current passing through the inductor of the EMI filter of the PFC converter in both low and high line voltages.

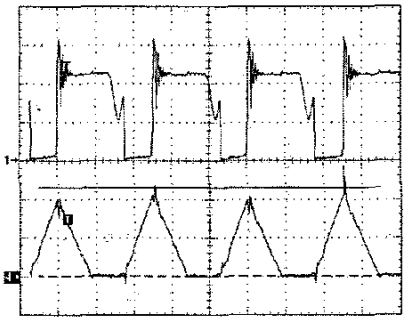

(a)

(b)

Fig. 7. Switch voltage and inductor current, from top to down, for (a) power and (b) sense pulses (V_{line} =90 Vac).

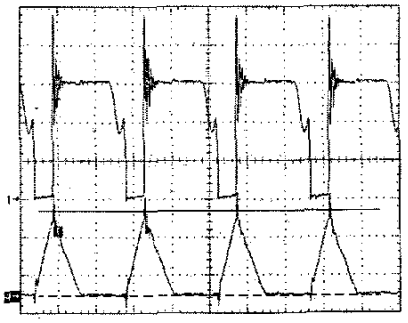

(a)

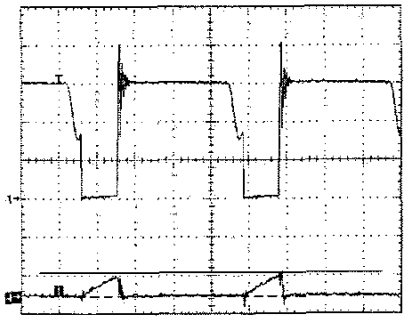

(b)

Fig. 8. Switch voltage and inductor current, from top to down, for (a) power and (b) sense pulses (V_{line} =130 Vac).

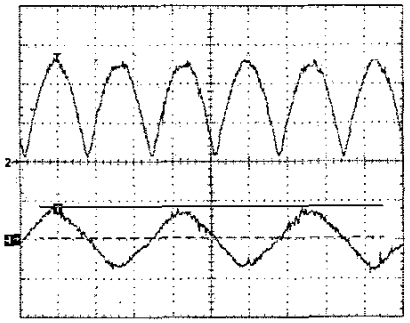

(a)

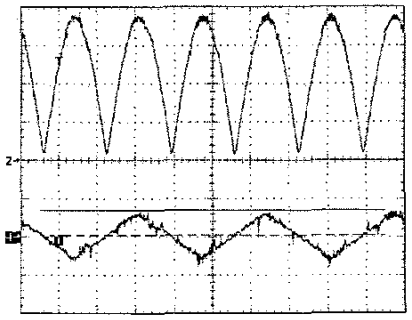

(b)

Fig. 9. Rectified voltage and input current of the EMI filter, from top to down, (a) line voltage=90 Vac and (b) line voltage=130 Vac .

VII. SMART-SKIP MODE

As has already been mentioned, the peak inductor current in a power pulse is k times the peak inductor current in a sense pulse; therefore, a sense pulse delivers $1/k^2$ as much power as a power pulse. A continuous stream of sense pulses thus delivers $100/k^2$ % of the full load. If the load is lighter than this level, the controller enters *Smart-Skip Mode*, when the circuit alternates between the sense pulses and no pulses at all.

The controller decides to enter smart-skip mode when the sense pulses reveal that the output voltage is remaining above the desired level, though no power pulses have been sent recently (Fig. 10(a)). The depth of the smart-skip mode (the ratio of skipped cycles to sense pulses) is increased or decreased according to the measured voltage and current in the skip-mode. The depth of the smart-skip mode needs to be reduced as the load increases (Fig. 10(b)).

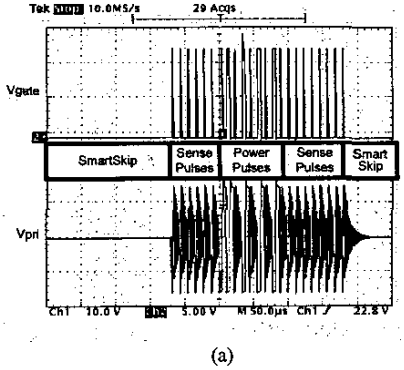

(a)

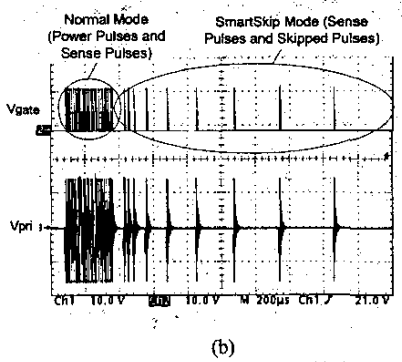

(b)

Fig. 10. (a) Experimental results of smart-skip, (b) the depth of smart-skip mode increasing with light load.

VIII. SOFT START

Fig. 11 depicts the experimental signal waveforms at start-up. The first power pulse shows a clean current ramp; but, the drain voltage reflects the fact that the transformer does not reset by the time the second pulse arrives and, thus, is operating in continuous conduction mode. This is also shown in the current on the second pulse, which starts at a non-zero value. However, the controller's peak current limiting causes the second power pulse to be much shorter than the first one. By the third cycle, the initial current has already fallen significantly due to the second cycle's shorter on time of the switch. This trend will continue until, in a few cycles, the initial current is zero and the converter is operating in discontinuous conduction mode.

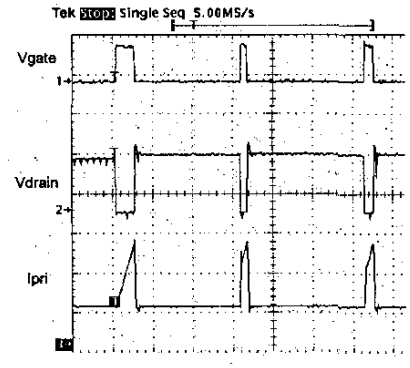

Fig. 11. Current limiting during start-up.

IX. CONCLUSION

DCM power converters have found their way into many applications. To address the challenge of designing controllers for this type of converters, this paper introduces the novel Power Pulse control theory. This new real time control method has several advantages over conventional techniques, such as robustness, accuracy, and fast transient response. Simulations as well as experimental results completely match with the theoretical concept.

ACKNOWLEDGEMENT

Financial support of iWatt Corporation for this work is gratefully acknowledged.

REFERENCES

[1] I. Gadoura, K. Zenger, T. Suntio, and P. Vallittu, "New methodology for design, analysis, and validation of DC/DC converters based on advanced controllers," in *Proc. 21st International Telecommunication Energy Conf.*, Copenhagen, Denmark, June 1999, pp. 6-9.

[2] T. W. Martin and S. S. Ang, "Digital control for switching converters," in *Proc. IEEE International Symposium on Industrial Electronics*, vol. 2, 1995, pp. 480-484.

[3] P. T. Tang and C. K. Tse, "Design of DSP-based controller for switching power converters," in *Proc. IEEE TENCON Digital Signal Processing Applications*, vol. 2, 1996, pp.889-894.

[4] R. R. Boudreaux, R. M. Nelms, and J. Y. Hung, "Simulation and modeling of a DC-DC converter controlled by an 8-bit microcontroller," in *Proc. IEEE 12th Annual Applied Power Electronics Conf.*, vol. 2, 1997, pp. 963-969.

[5] C. H. Chan and M. H. Pong, "DSP controlled power converter," in *Proc. International Conference on Power Electronics and Drive Systems*, vol. 1, 1995, pp. 364-369.

[6] Y. Duan and H. Jin, "Digital controller design for switch mode power converters," in *Proc. IEEE 14th Annual Applied Power Electronics Conf.*, vol. 2, 1999, pp. 967-973.

[7] R. E. Strawser, B. T. Nguyen, and M. K. Kazimierczuk, "Analysis of a buck PWM DC-DC converter in discontinuous conduction mode," in *Proc. IEEE National Aerospace and Electronics Conf.*, 1994, pp. 35-42.

[8] J. Chen and K. D. T. Ngo, "Alternate forms of the PWM switch model in discontinuous conduction mode DC-DC converters," *IEEE Trans. on Aerospace and Electronic Sys.*, vol. 37, no. 2, pp. 754-758, April 2001.

[9] J. Chen and K. D. T. Ngo, "Simplified analysis of PWM converters operating in discontinuous conduction mode using alternate forms of the PWM switch models," in *Proc. IEEE Southeastcon*, 2000, pp. 505-509.

[10] M. Telefus, A. Collmeyer, D. Wong, and D. Manner, "Switching power converter with gated oscillator controller," *US Patent No. 6,275,018*, Assignee: iWatt Corporation.

[11] M. Telefus, D. Wong, and C. Geber, "Operating a power converter at optimal efficiency," *US Patent No. 6,304,473*, Assignee: iWatt Corporation.